Applied Surface Science 255 (2009) 9592–9596

Contents lists available at ScienceDirect

Applied Surface Science

journal homepage: www.elsevier.com/locate/apsusc

Molecular dynamics simulation of femtosecond ablation and spallation with different interatomic potentials

V.V. Zhakhovskii [a,*], N.A. Inogamov [c], Yu.V. Petrov [c], S.I. Ashitkov [b], K. Nishihara [a]

[a] Institute of Laser Engineering, Yamada-oka 2-6, Suita, Osaka 565-0871, Japan
[b] Joint Institute of High Temperature RAS, 13/19 Izhorskaya Street, Moscow 125412, Russia
[c] L.D.Landau Institute for Theoretical Physics RAS, Chernogolovka 142432, Russia

ARTICLE INFO

Article history:
Available online 21 April 2009

PACS:
02.70.Ns
79.20.Ds
52.38.Mf

Keywords:
Molecular dynamics
EAM potential
Femtosecond laser ablation

ABSTRACT

Fast heating of target material by femtosecond laser pulse (fsLP) with duration $\tau_L \sim 40-100$ fs results in the formation of thermomechanically stressed state. Its unloading may cause frontal cavitation of subsurface layer at a depth of 50 nm for Al and 100 nm for Au. The compression wave propagating deep into material hits the rear-side of the target with the formation of rarefaction wave. The last may produce cracks and rear-side spallation. Results of MD simulations of ablation and spallation of Al and Au metals under action fsLP are presented. It is shown that the used EAM potentials (Mishin et al. and our new one) predict the different ablation and spallation thresholds on absorbed fluence in Al: ablation $F_a = 60\{65\}$ mJ/cm^{2}and spallation $F_s = 120\{190\}$ mJ/cm^2, where numbers in brackets { } show the corresponding values for Mishin potential. The strain rate in spallation zone was 4.3×10^9 1/s at spallation threshold. Simulated spall strength of Al is 7.4{8.7} GPa, that is noticeably less than 10.3{14} GPa obtained from acoustic approximation with the use of velocity pullback on velocity profile of free rear surface. The ablation threshold $F_a \approx 120$ mJ/cm^2 and crater depth of 110 nm are obtained in MD simulations of gold with the new EAM potential. They agree well with experiment.

1. Introduction

The ultrashort laser-matter interaction with pulse duration less than 1 ps and moderate fluence ~ 1 J/cm^2 is important for fundamental physics of fast processes, warm dense matter physics as well as for a wide range of industrial applications [1–3]. The depth of photon (or multiphoton for intensity $> 10^{12}$ W/cm^2) absorption can be a few nanometers in metals. As a result the fsLP may induce nanoscale phenomena in absorbing material without significant warming up and damage of the material surrounding the focal spot. The time and length scales of the processes involved provide an exceptional opportunity to apply MD simulation to study fundamental atomic-scale mechanisms of materials response to fsLP at the level of detail that is difficult or impossible to obtain from experiment.

There are two problems in MD approach. Firstly, it should be combined with another model capable of evaluating the electron and ion temperature in material as functions of position and time during several picoseconds from starting of absorption of fsLP. The works [2] propose such model. Secondly, for the problem of laser-matter interaction the appropriate interaction potential is a prime necessity to describe material properties realistically and adequately in wide range of pressure, temperature and density. For instance the much used embedded atom model (EAM) potentials of Mishin et al. [4] and Ercolessi–Adams [5] are well optimized for aluminum nearby standard conditions, but not for highly compressed and rarefied states peculiar to material under action of fsLP.

2. New analytical EAM potential

To simulate the behavior of aluminum crystal under action of strong compression and rarefaction waves we develop a new analytical EAM potential based on cold pressure curves evaluated from the density functional theory (DFT).

The common form of EAM potential is given by

$$E_{tot} = \sum_i F(n_i) + \sum_{i<j} V(r_{ij}), \quad n_i = \sum_{k \neq i} n(r_{ik}), \tag{1}$$

where $V(r_{ij})$ is a pair potential, $F(n_i)$ is an embedding energy of i-atom, and $n(r_{ik})$ is a density function. The both mentioned above EAM potentials [4,5] use a cubic spline representation of these

* Corresponding author. Tel.: +81 6 6879 8744.
E-mail address: basil@ile.osaka-u.ac.jp (V.V. Zhakhovskii).

0169-4332/$ – see front matter © 2009 Elsevier B.V. All rights reserved.
doi:10.1016/j.apsusc.2009.04.082

functions. Here we introduce an analytical EAM potential for aluminum as follows

$$x = a_1 r^2, \quad x_c = a_1 r_c^2,$$

$$V(r) = \left(\frac{1}{x} - a_2\right)(x - x_c)^{10}((x - x_c)^6 + a_3 x^6) \tag{2}$$

$$F(n) = \frac{b_1 n(b_2 + (b_3 + n)^2)}{1 + b_4 n} \tag{3}$$

$$n(r) = \frac{c_1 (r^2 - r_c^2)^2}{1 + (c_2 r^2)^3} \tag{4}$$

where $r_c = 0.6875$ nm is chosen as a cutoff radius.

The fitting parameters a_N, b_N, c_N were found by minimizing the sum of deviations from components of cold pressure tensor evaluated by using the ABINIT code [6] and the experimental Al properties at $T = 0$ K taken from [5]. The Al lattice constant is 0.4032 nm, cohesive energy −324.19 kJ/mol, and bulk modulus 80.9 GPa. These experimental points have the largest weights in the fitting procedure.

The calculations of cold pressure curves are based on the DFT with local density approximation and by using of the Troullier–Martins pseudopotentials for Al, code is available on [6]. The plane-wave cutoff energy was 871 eV. The EAM potential has two well-known invariant transformations, thus two additional conditions are imposed on fitting parameters. First is $n_{eq} = 1$ for an equilibrium crystal at $P = T = 0$, and second is $F'(n_{eq}) = 0$. These conditions are satisfied exactly by parameters presented in Table 1, where nm as unit of length and kJ/mol as unit of energy are used. The powers in Eqs. (2)–(4) were also adjusted to fit data better. The new potential with fitting parameters from Table 1 reproduces the Al properties with good accuracy. It gives 0.4032 nm for Al lattice constant, −324.258 kJ/mol for cohesive energy, 81.57 GPa for Al bulk modulus at $P = T = 0$, and 940 K for melting point.

The cold pressure components $P(V/V_0, T = 0)$ evaluated by ABINIT as functions of relative uniform and uniaxial ⟨1 0 0⟩ compression-stretching are shown by symbols in Fig. 1. The calculated cold pressure curves represented by lines in Fig. 1 indicate the significant difference in the largest stress σ^* at which Al ruptures. Mishin potential overestimates σ^* about 4 GPa for the uniaxial ⟨1 0 0⟩ stretching of ideal Al crystal. As we show below it results in higher spall strength than one predicted by MD simulation with the new Al EAM potential.

For gold the similar form of EAM potential as in Eqs. (2)–(4) and the same minimization procedure were used to find the fitting parameters a_N, b_N, c_N and powers of new Au EAM potential, see Table 1. The pair potential function Eq. (2) is replaced by Eq. (5) optimized for Au:

$$V(r) = \left(\frac{1}{x} - a_2\right)(x - x_c)^{10}((x - x_c)^{18} + a_3) \tag{5}$$

The new potential gives 0.4065 nm for Au lattice constant, −367.609 kJ/mol for cohesive energy, 179.4 GPa as a bulk modulus at $P = T = 0$, and ∼1330 K for melting point of Au. Fig. 2 shows the cold pressure components evaluated by ABINIT and new Au EAM potential. The new EAM potentials provide also good fits of pressure curves evaluated by ABINIT and Rose EOS [7] for large stretching as indicated in Figs. 1 and 2 as well as for large compression ratio V/V_0 up to 0.5 and pressure ∼1000 GPa.

Table 1
EAM potentials Eqs. (2)–(5) for aluminum and gold.

N	a_N in $V(r)$ for Al	a_N in $V(r)$ for Au
1	2.9275228176598036	2.7471581015136728
2	5.1028014804162156	5.3593750000000000
3	111.37742236893590	3.2500000000000000
N	b_N in $F(n)$ for Al	b_N in $F(n)$ for Au
1	8.1106000931637006	8.2311259601633768
2	−334.57493744623503	−382.38931538388255
3	14.868297626731845	16.250071667347235
4	1.6080953931773090	1.4586663896542300
N	c_N in $n(r)$ for Al	c_N in $n(r)$ for Au
1	0.58002942432410864	3.0697898737897571
2	8.2981185422063639	20.750105835621902

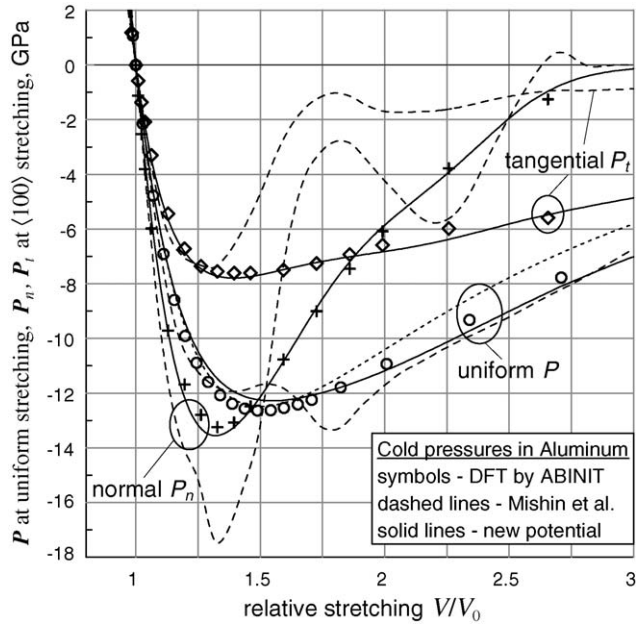

Fig. 1. The cold uniform pressure P, normal P_n and tangential P_t components of pressure tensor obtained by new Al EAM potential, Mishin et al. [4], DFT ABINIT [6], and from the EOS by Rose et al. [7](dotted line).

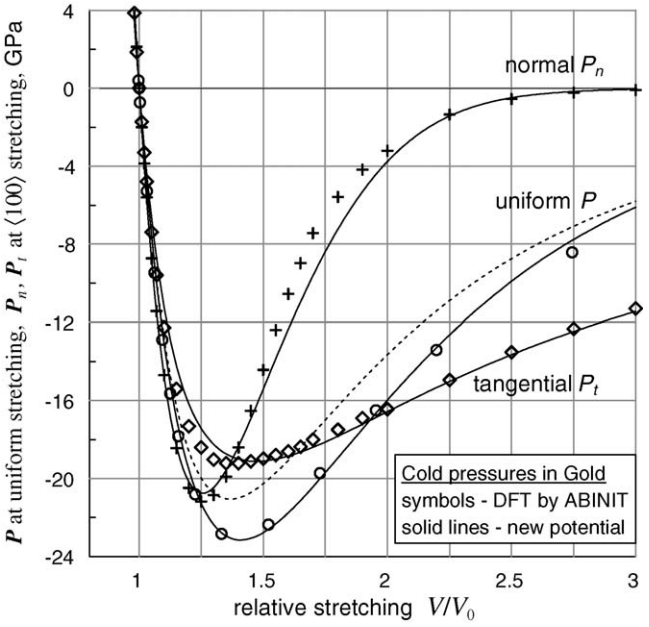

Fig. 2. The cold pressure $P(V/V_0, T = 0)$ components obtained by new Au EAM potential, DFT ABINIT, and from Rose's EOS (dotted line).